

Isotropic, aberration-corrected light sheet microscopy for rapid high-resolution imaging of cleared tissue

Authors

Mostafa Aakhte^{1*}, Gesine F. Müller¹, Joe Li², Kurt R. Weiss³, Lennart Roos^{4,5,6,7}, Aleya M. Diniz^{4,5,7,8}, Jan Wenzel^{9,10}, Markus Schwaninger^{9,10}, Tobias Moser^{4,5,6,7,8} and Jan Huiskens^{1,2,7,10*}

Affiliations

¹Multiscale Biology, Department of Biology and Psychology, University of Göttingen, Göttingen, Germany.

²Morgridge Institute for Research, Madison, WI, USA

³Department of Biochemistry, University of Wisconsin, Madison, WI, USA

⁴Institute for Auditory Neuroscience and InnerEarLab, University Medical Center Göttingen, Göttingen, Germany

⁵Else-Kröner-Fresenius Center for Optogenetic Therapies, University Medical Center Göttingen, Göttingen, Germany

⁶Department of Otorhinolaryngology, University Medical Center Göttingen, Göttingen, Germany

⁷Cluster of Excellence "Multiscale Bioimaging: from Molecular Machines to Networks of Excitable Cells" (MBExC), University of Göttingen, Göttingen, Germany

⁸Auditory Neuroscience and Synaptic Nanophysiology Group, Max Planck Institute for Multidisciplinary Sciences, Göttingen, Germany

⁹Institute of Experimental and Clinical Pharmacology and Toxicology, Center of Brain, Behavior and Metabolism, University of Lübeck, Lübeck, Germany

¹⁰German Research Centre for Cardiovascular Research (DZHK), partner site Hamburg/Lübeck/Kiel and Göttingen, Germany

*e-mail: mostafa.aakhte@uni-goettingen.de, jan.huiskens@uni-goettingen.de

Supplementary materials

Supplementary Note1

Supplementary Fig1. **Resolution calculation for multi-immersion objective lens.**

Supplementary Fig2. **3D rendering of the cleared tissue optical setup.**

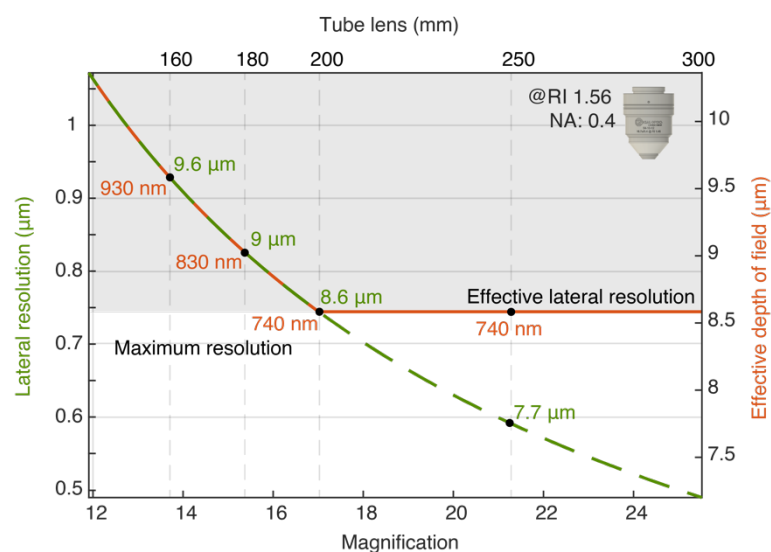
Supplementary Fig3. **Mouse brain preparation for imaging.**

Supplementary Fig4. **Electronics components and their expected electrical waveforms.**

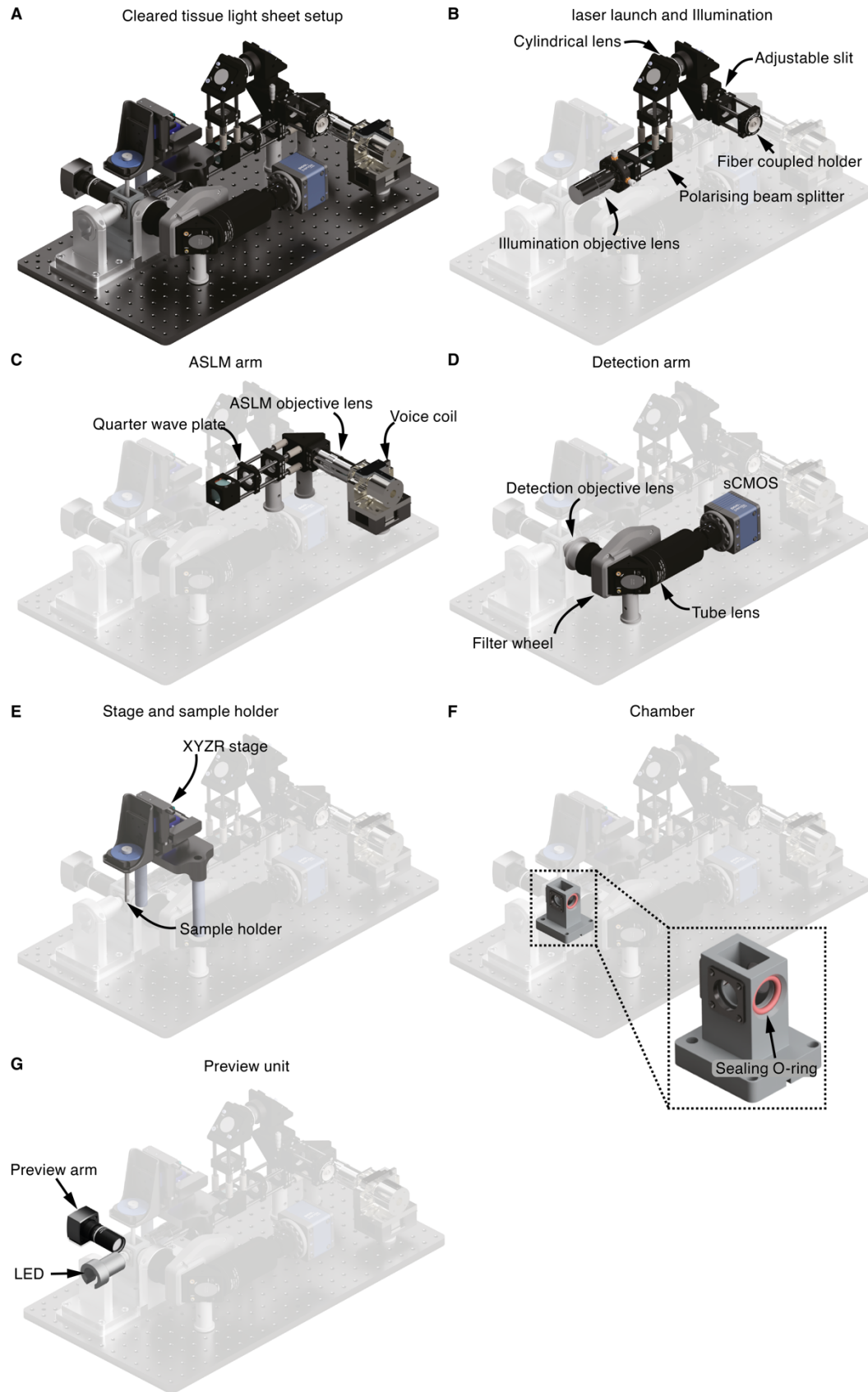
Supplementary Table1. **Comparison between the different tested sCMOS cameras.**

Supplementary Note1

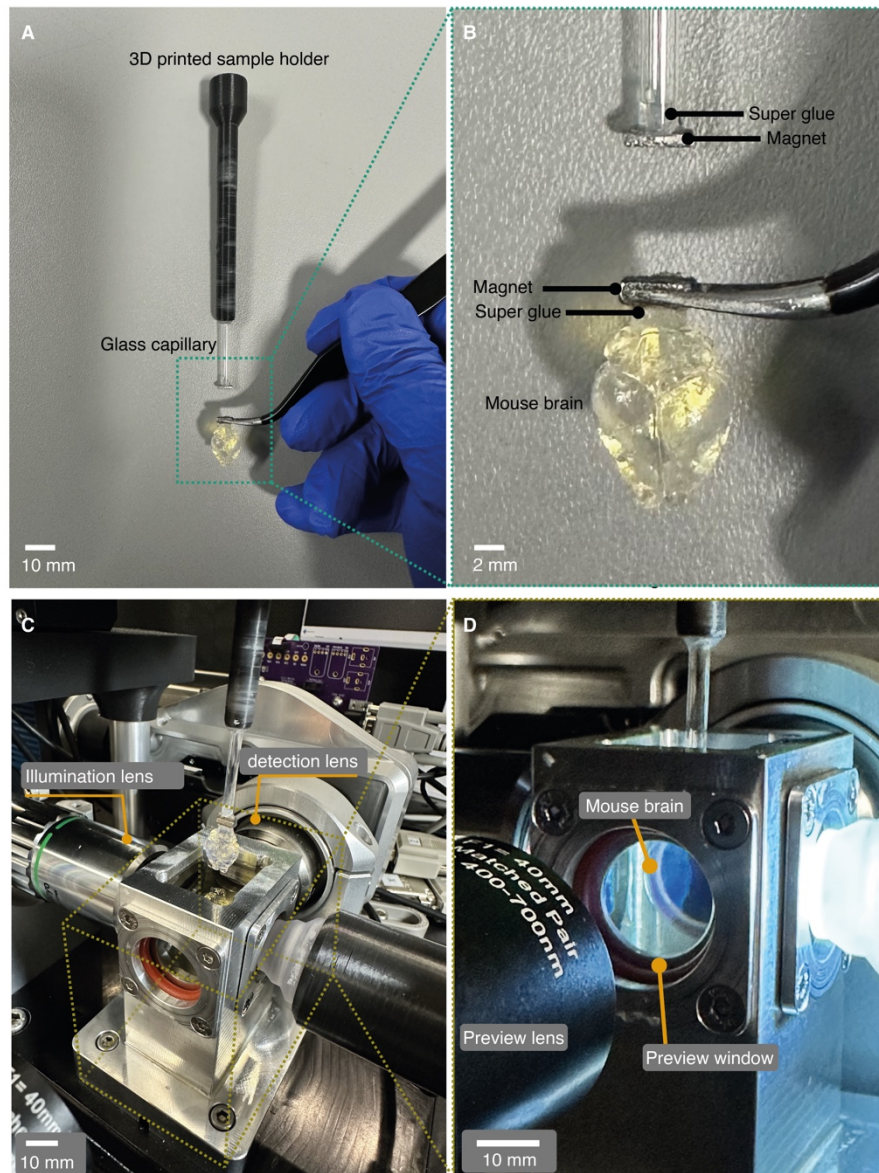
The theoretical resolution and imaging depth of field (DOF) are presented in this section for the ASI objective lens with NA 0.4. The calculated parameters are sorted by varying the tube lens and magnification to make it easier to follow the resolution and DOF behavior (**Supplementary Fig. 1**). The tube lenses are chosen from the 160–300 mm focal length range, which provide magnifications of 13–25 \times . For tube lenses with focal lengths less than 200 mm, the lateral resolution and magnification increase as the focal length of the tube lens approaches 200 mm. Following that, the resolution remains constant as it is limited by the camera's pixel pitch of 6.5 μm . The highest resolution achievable with the objective lens is then given by the objective lens' NA. For instance, for a refractive index of 1.56 and a tube lens of $f=200$ mm or longer, the highest theoretical achievable resolution for the ASI lens with an NA of 0.4 is 740nm. The depth of field (DOF) of the objective lens decreases as the focal length of the tube lenses is increased. This is because the DOF and magnification have an inverse relationship. Thus, increasing the magnification decreases the DOF. As a result, the optimal tube lenses for the ASI lenses have a focal length of 200 mm to achieve the highest resolution possible.



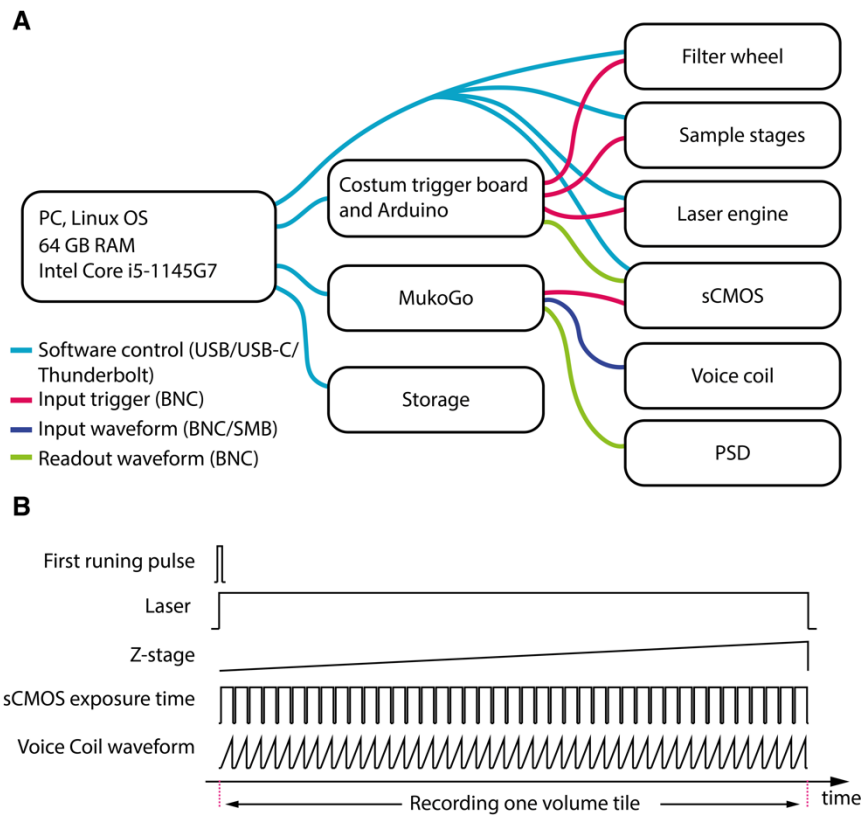
Supplementary Fig. 1. Resolution considerations for multi-immersion objective lens. Lateral resolution and effective depth of field for the ASI lens with NA 0.4 are calculated in relation to the magnification and focal length of the tube lens. The solid orange and dashed green lines represent the lateral resolution and DOF, respectively. The grey area indicates the achievable resolution with a camera pixel pitch of 6.5 μm .



Supplementary Fig. 2. 3D rendering of the cleared tissue optical setup. (A) 3D rendering of the entire setup. (B) Laser launch and illumination arm. (C) ASLM arm. (D) Detection arm. (E) Sample stage and holder. (F) Chamber. (G) Preview unit. The base plate's size is 30x60 cm².



Supplementary Fig. 3. Mouse brain preparation for imaging. **A**, A cleared mouse brain is glued to a magnet using super glue and a 3D-printed sample holder secures a glass capillary with another magnet at its tip. **B**, An enlarged view of the mouse brain shown in A. **C**, An illumination objective lens, a detection objective lens, and an LED with a 3D-printed holder surround a chamber filled with ECI. **D**, The cleared mouse brain inside the chamber is visible through a preview window facing the preview lens.



Supplementary Fig. 4. Electronics components and their electrical waveforms. (A) The microscope is run by a small Linux computer. All components are either directly connected to the computer via USB or connected to trigger boards such as a custom board, Arduino, and MokuGo. The recorded data is streamed to a solid-state drive (SSD). (B) The microscope's components are started by a user command and a trigger board sends signals to the other components such as Laser, Z-stage, sCMOS, and voice coil.

Supplementary table 1. Comparison between the different tested sCMOS cameras.

sCMOS parameters in light sheet mode	pco.panda 4.2	Hamamatsu Orca-Fusion	pco.edge 10bi
Maximum frame rate (Hz)	40	100	120
Achieved frame rate in ASLM mode (Hz)	32	84	100
Exposure line (μ s)	12.136	4.868	6.84
Chip size (pixel)	2048x2048	2304x2304	4416x2368
Used chip (pixel)	2048x2048	2048x2048	2368x2368
Effective FOV (μ m x μ m)	780x780 (TL: 200mm)	780x780 (TL: 200mm)	625x625 (TL: 200mm) 750X750 (TL:160mm)
Volume imaging speed of 1mm ³ (4000 images)	2.2 min	45 sec	32 sec
Camera connection	USB-C	Frame grabber	Frame grabber